

# Using Observations to Constrain the Yield Curve, Flow Rule and Mechanical Strength of Sea Ice

Bruno Tremblay

Damien Ringeisen, Mathieu Plante, Amelie Bouchat, Nils Hutter, Martin Losch

The Future of Earth System Modeling: Polar Climate

Nov 28-30, 2018

Caltech, Keck Center, Pasadena

Funded by: ArcTrain - CanSISE



# Sea Ice Momentum Equation

The diagram illustrates the Sea Ice Momentum Equation, showing the relationship between various forces and the rate of change of momentum. The equation is presented as:

$$\rho_i h \frac{Du}{Dt} = -\rho_i h f \hat{k} \times u + \tau_a - \tau_w - \rho_i h g \nabla H_d + \nabla \cdot \sigma$$

Each term in the equation is associated with a physical process, indicated by blue arrows:

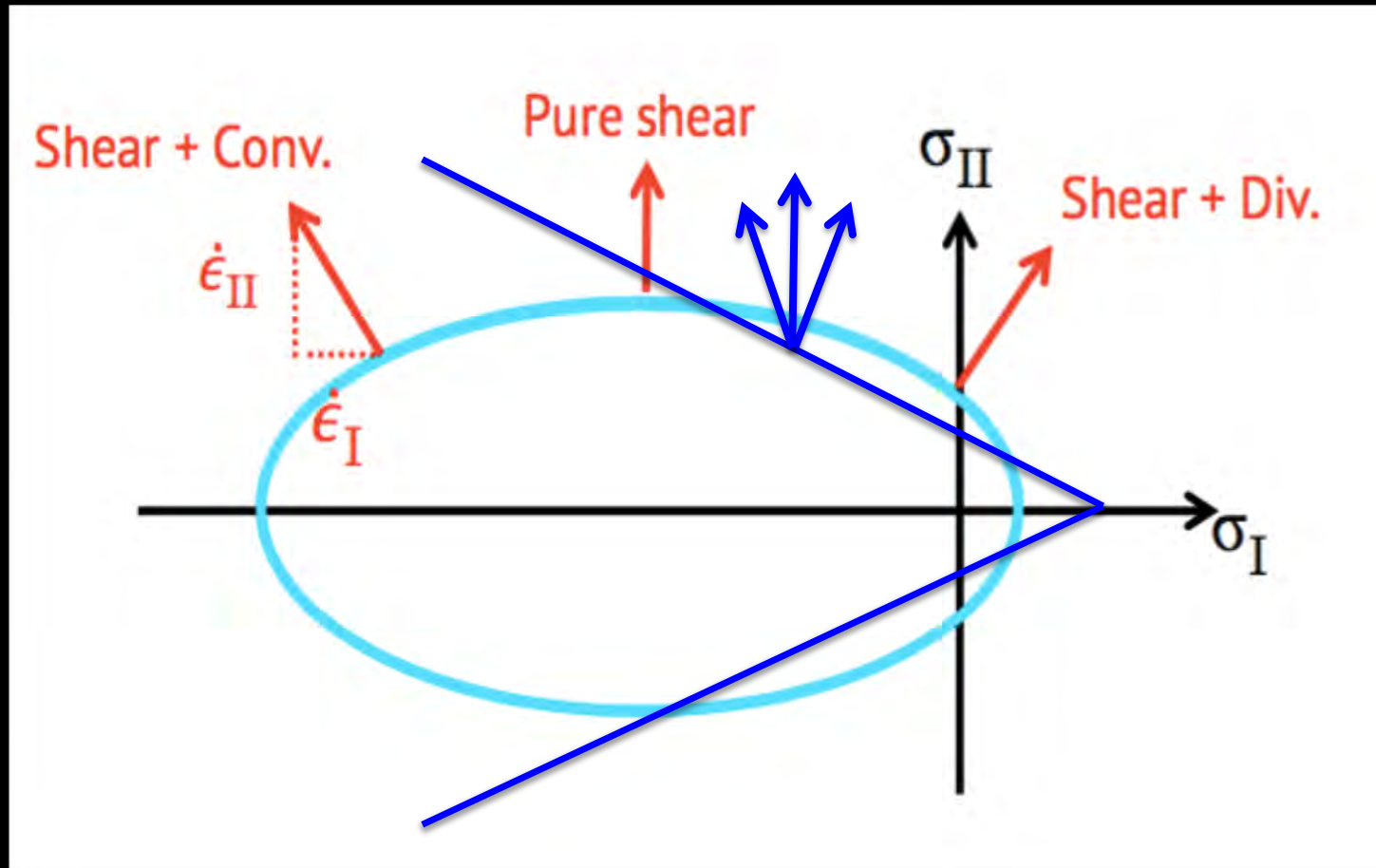
- inertial**: Points to the left-hand side term  $\rho_i h \frac{Du}{Dt}$ .
- Coriolis**: Points to the term  $-\rho_i h f \hat{k} \times u$ .
- air drag**: Points to the term  $\tau_a$ .
- water drag**: Points to the term  $-\tau_w$ .
- SSTilt**: Points to the term  $-\rho_i h g \nabla H_d$ .
- rheology**: Points to the term  $\nabla \cdot \sigma$ .

# Constitutive Relations

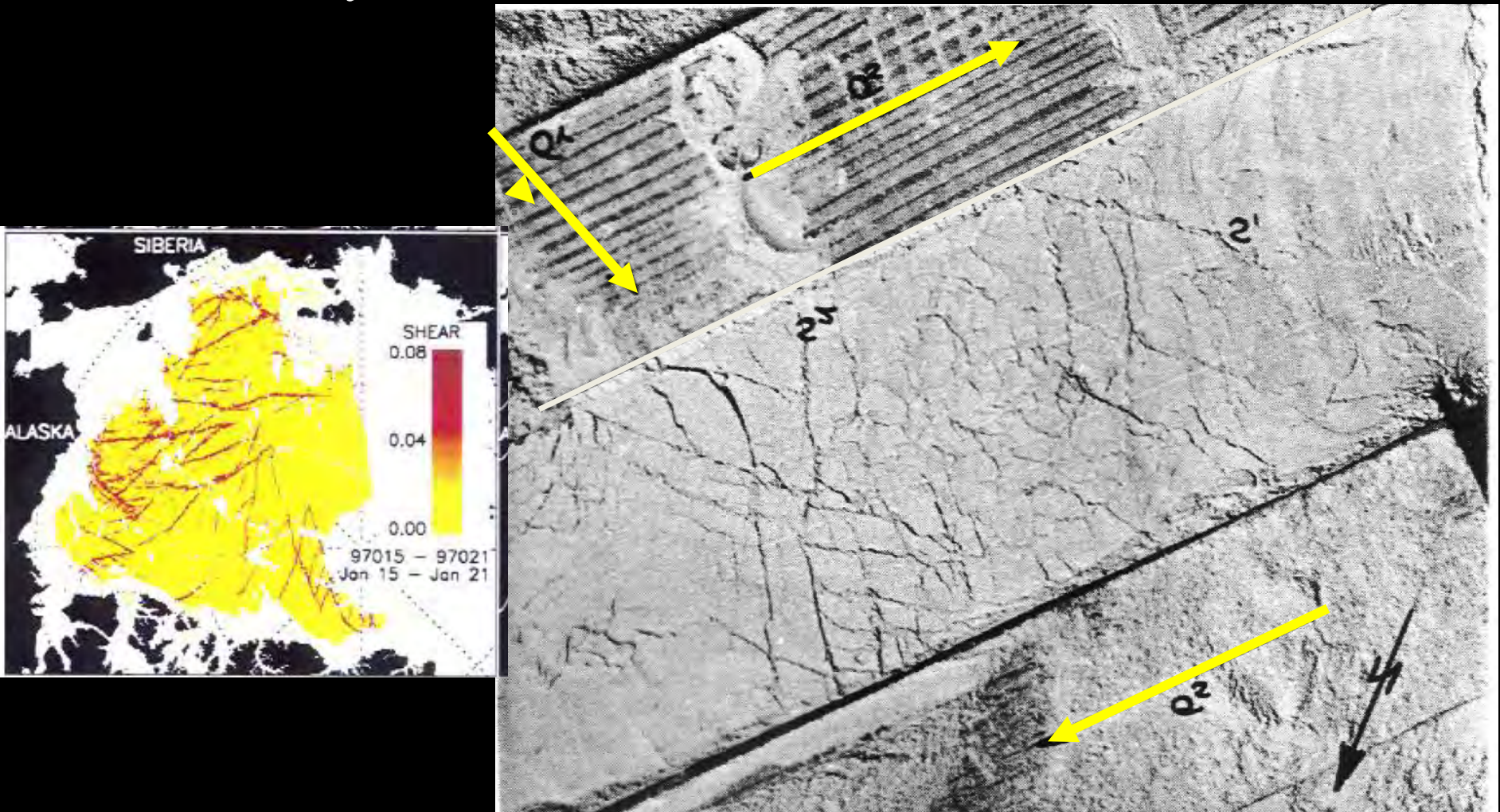
- Elastic
- Viscous (8 days)
- Plastic

# Plasticity

## Yield Curve and Flow Rules

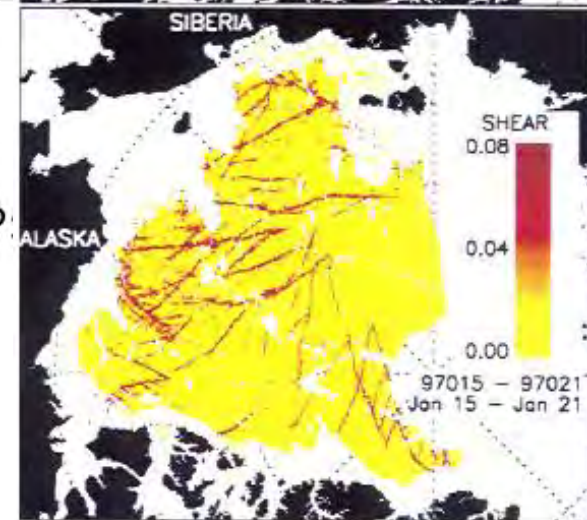
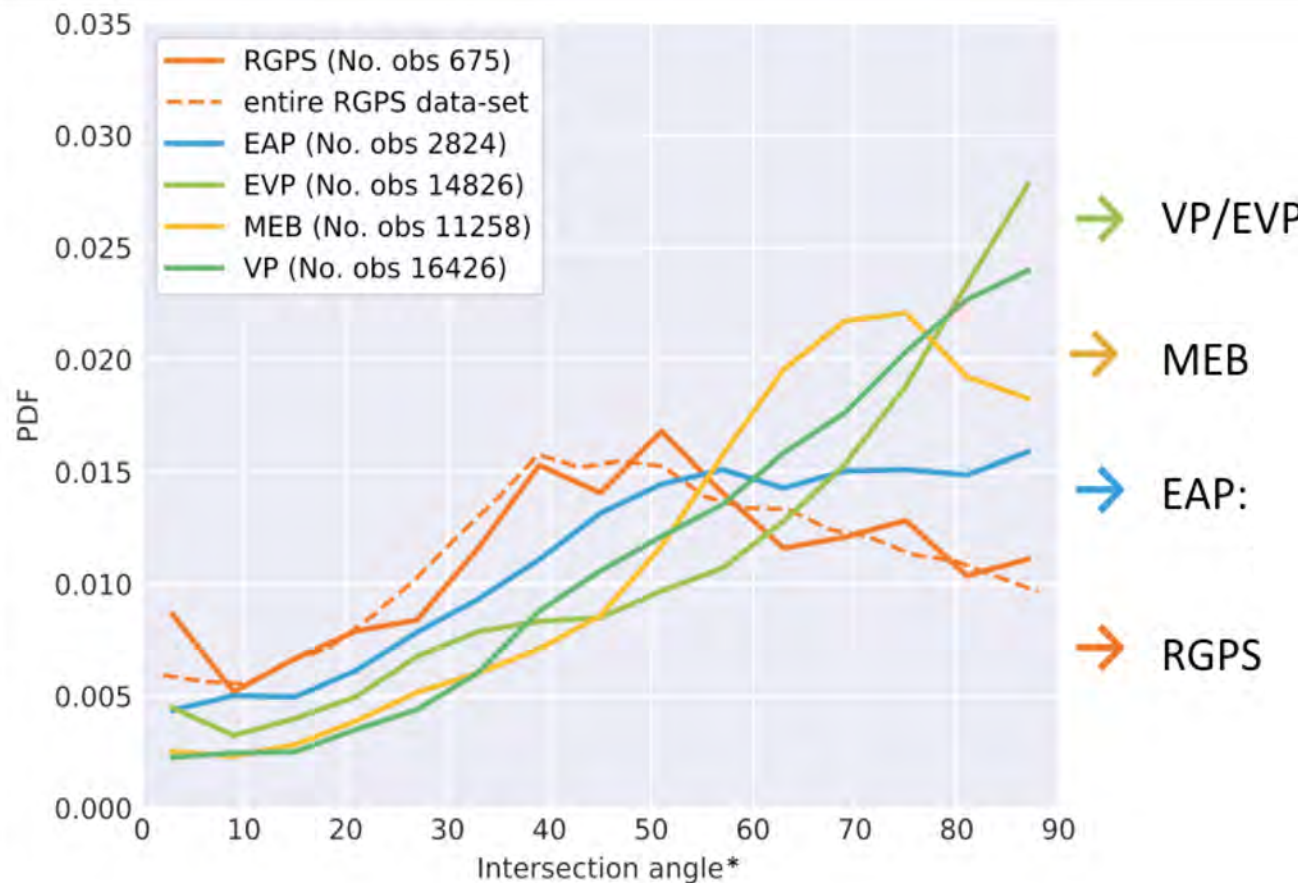


# Clay under shear deformation

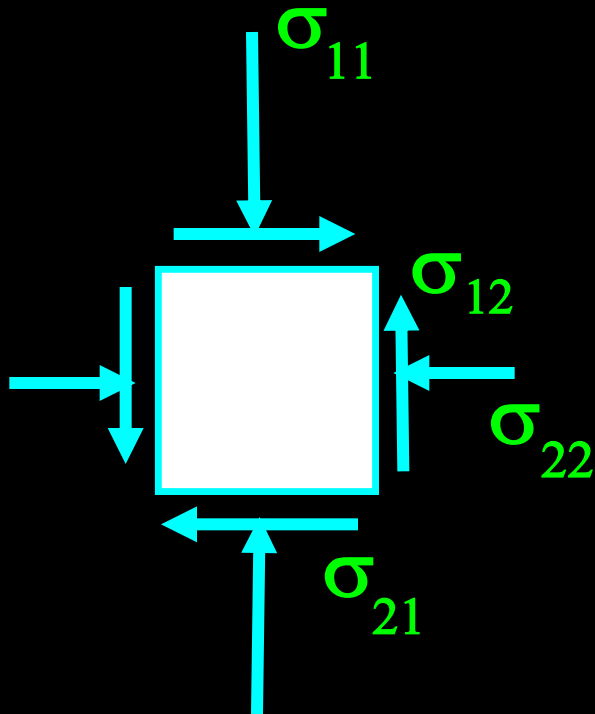




# Intersection of Fracture Lines

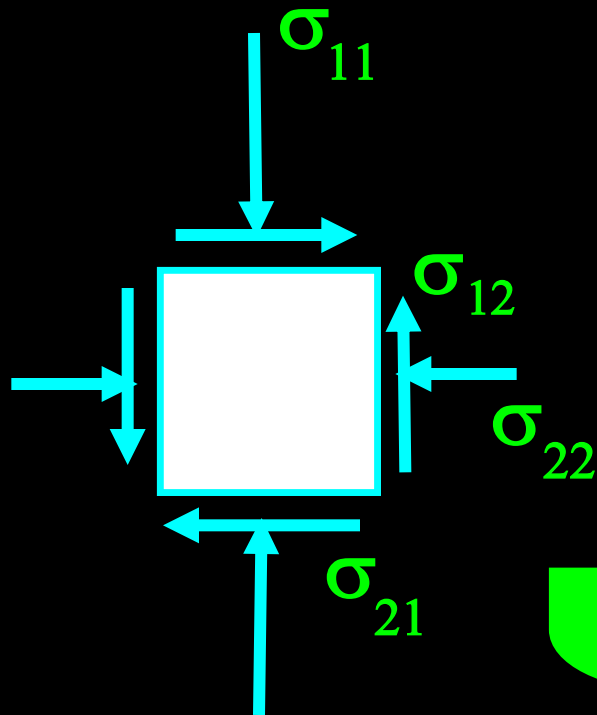


# Stress State



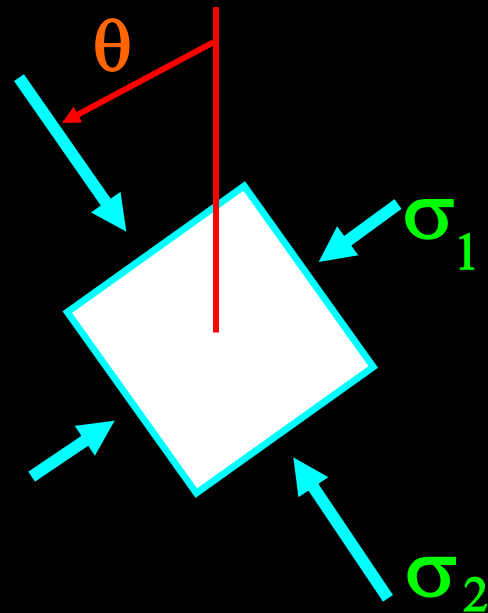
$$\begin{bmatrix} \sigma_{11} & \sigma_{12} \\ \sigma_{21} & \sigma_{22} \end{bmatrix}$$

# Stress State



$$\begin{bmatrix} \sigma_{11} & \sigma_{12} \\ \sigma_{21} & \sigma_{22} \end{bmatrix}$$

**Principal  
Stresses**



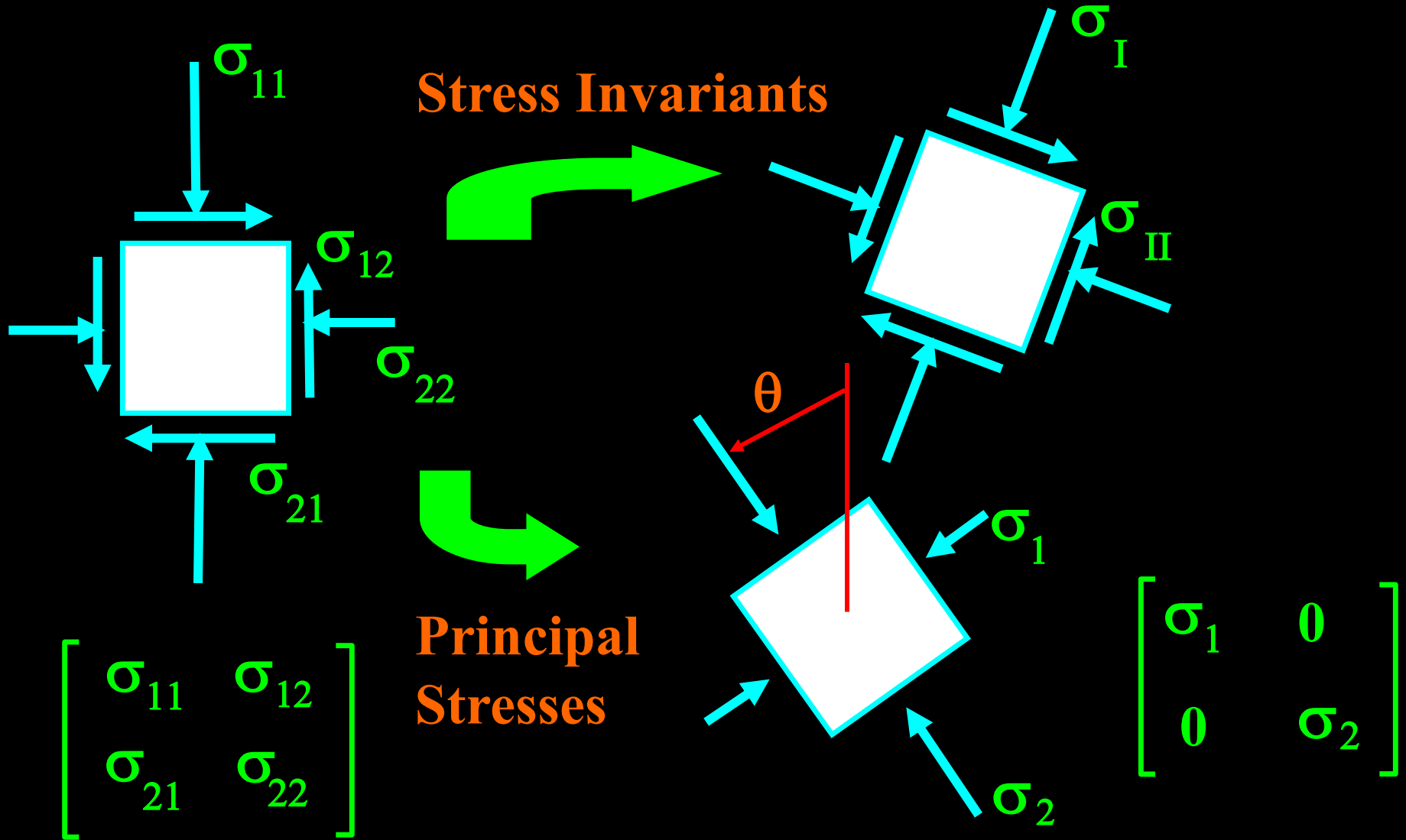
$$\begin{bmatrix} \sigma_1 & 0 \\ 0 & \sigma_2 \end{bmatrix}$$



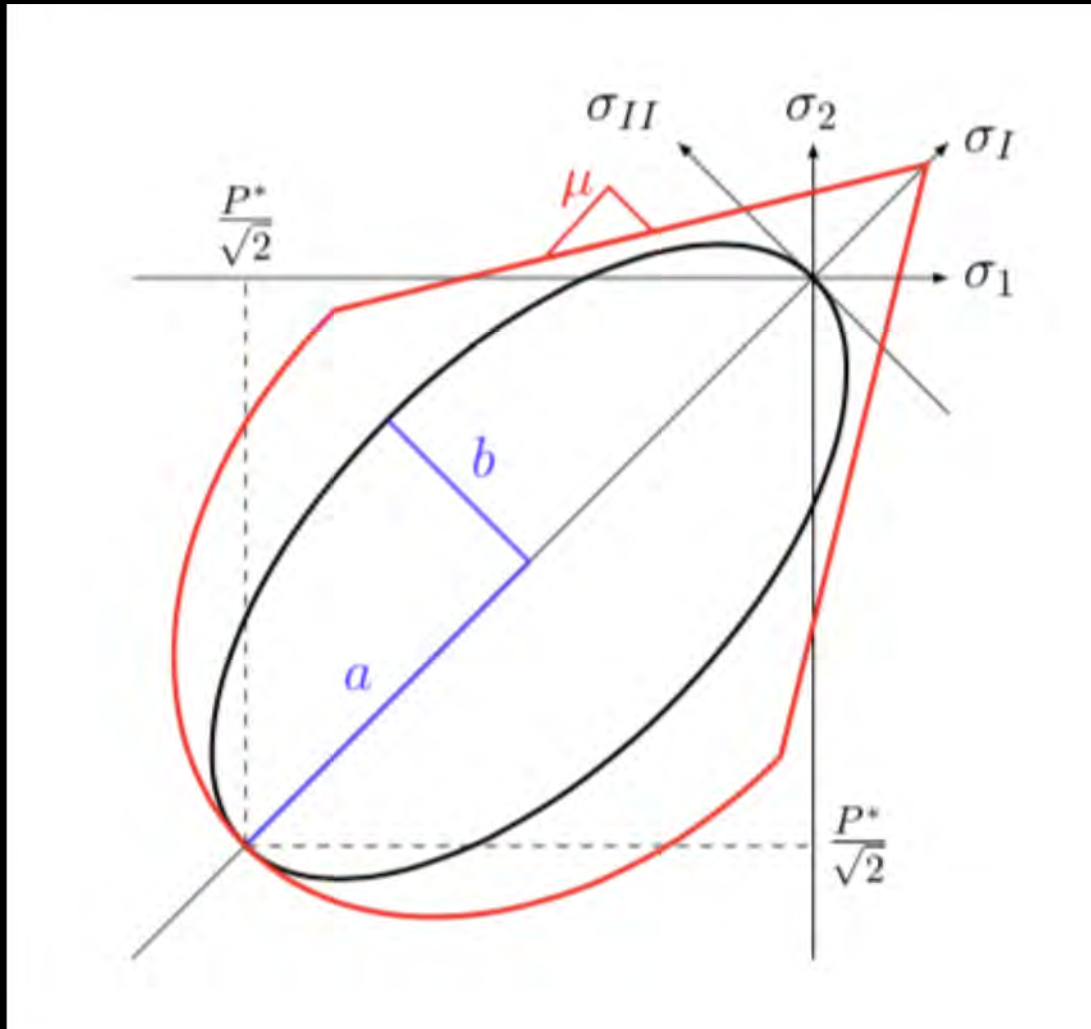
# Stress State

**Stress Invariants**

**Principal Stresses**



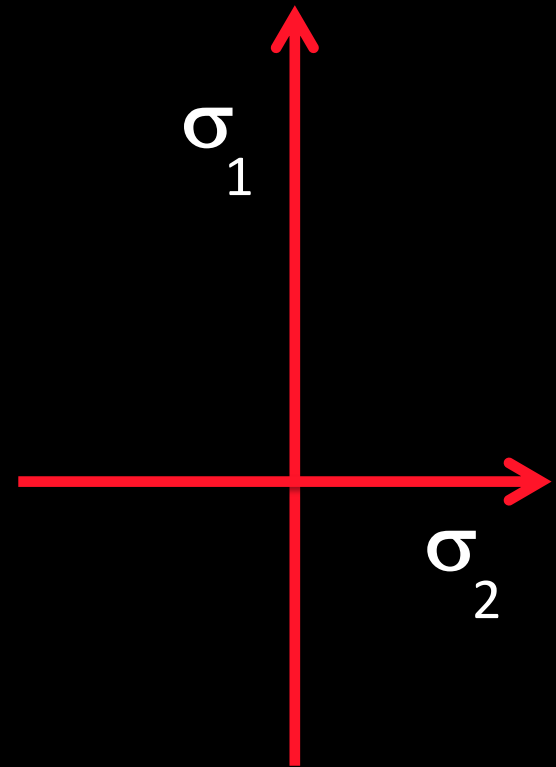
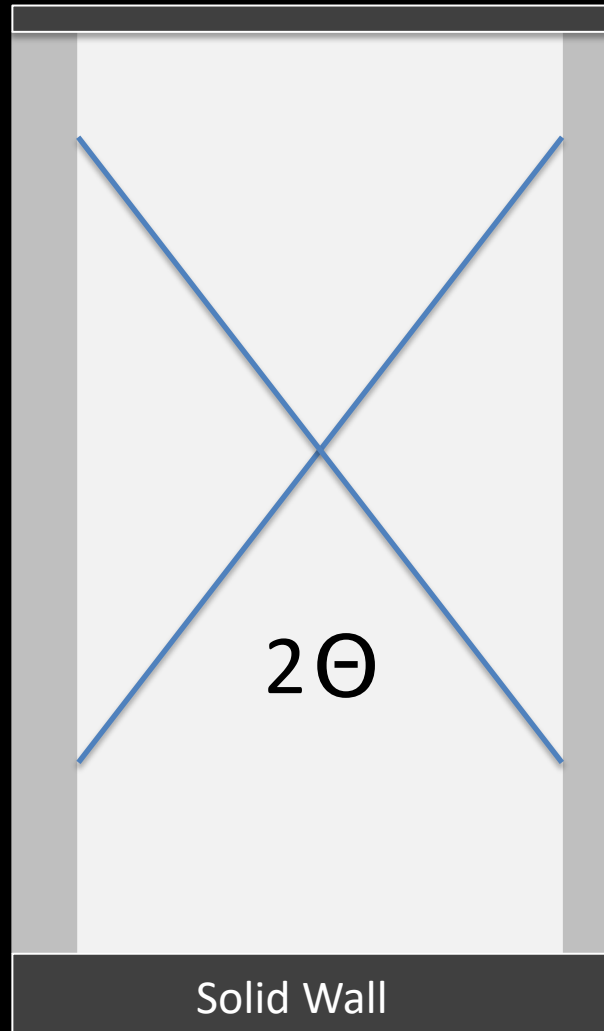
# Two Yield Curves



# Experimental Set-Up

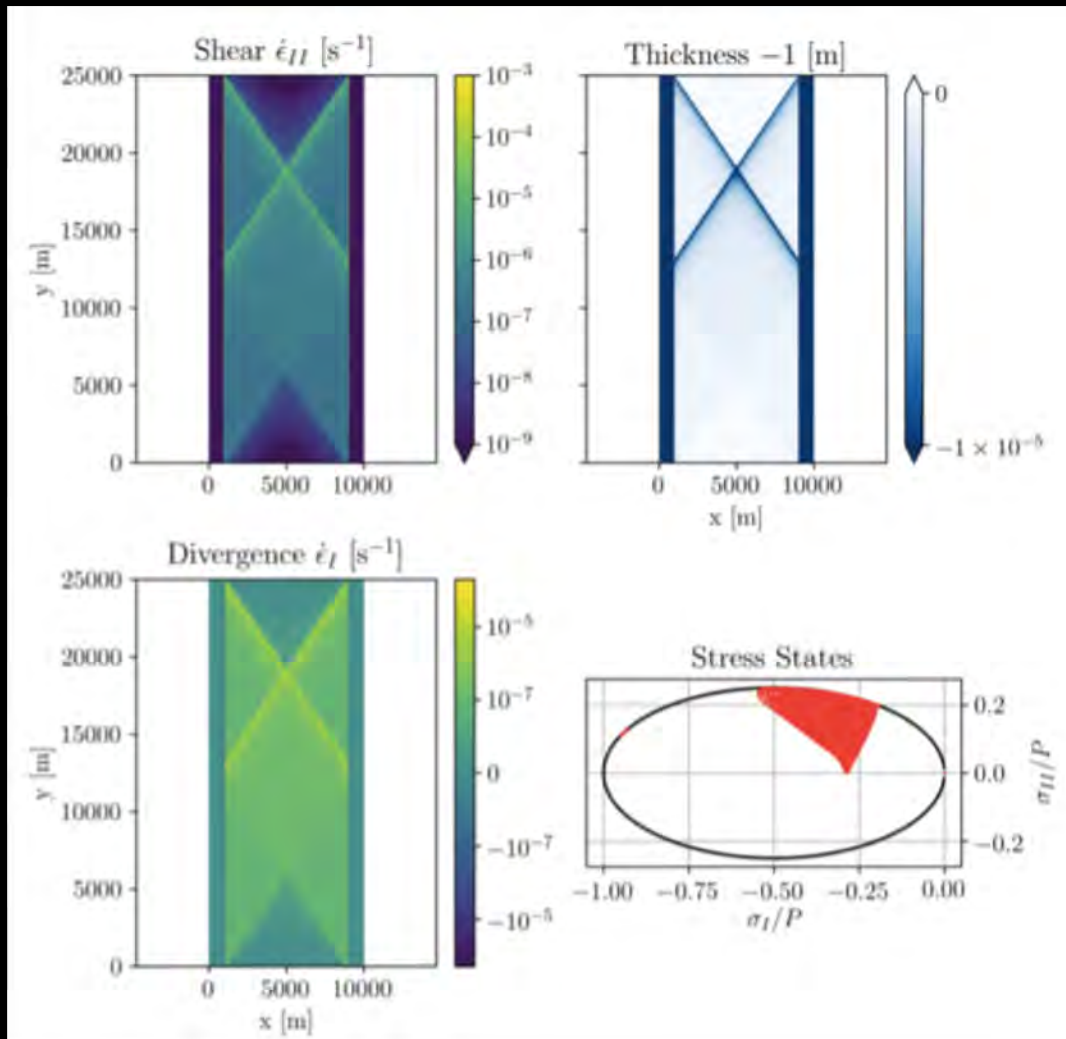
Prescribe Strain rate

8 km x 25 km  
 $dx = 25$  m



# Axial Loading Test

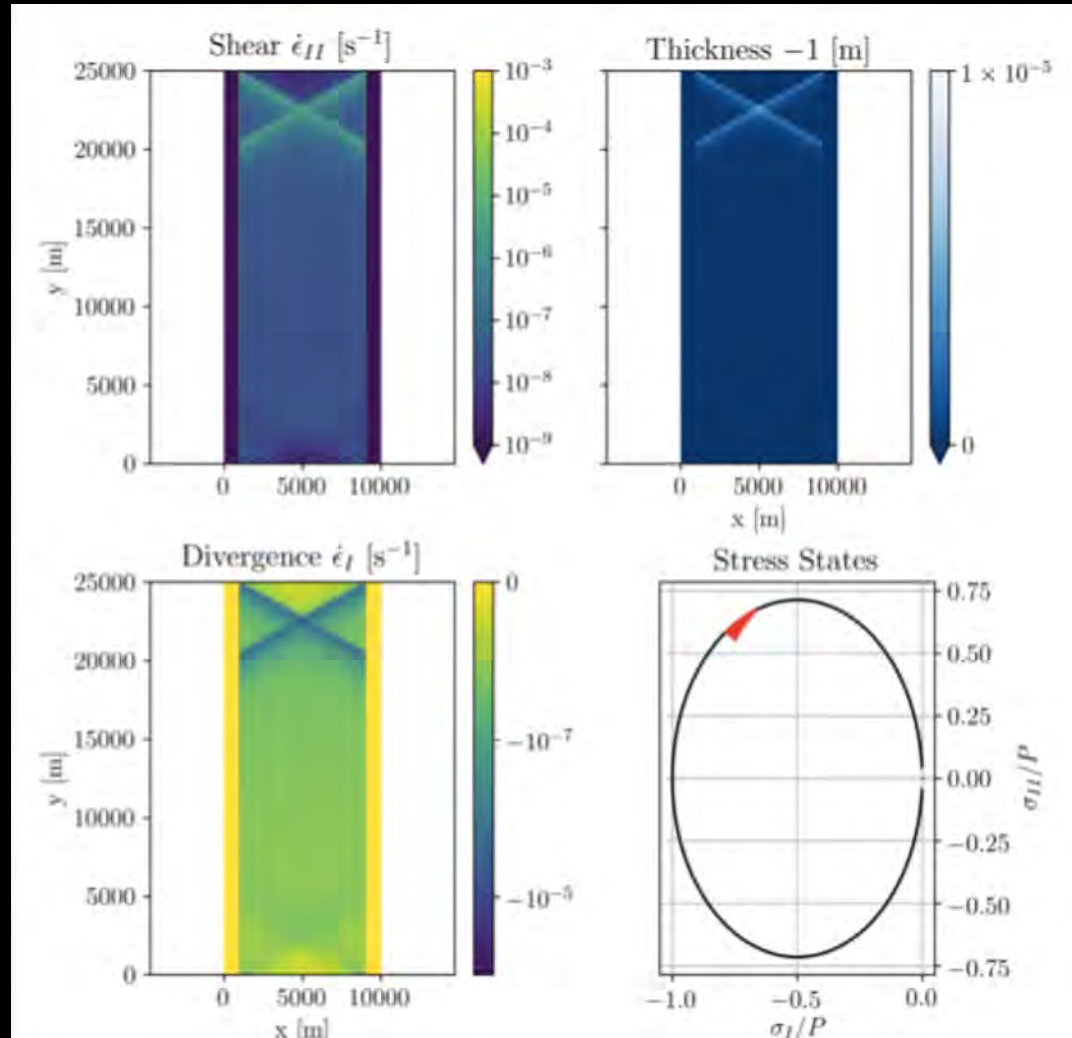
Control Run (e=2)



34 degrees

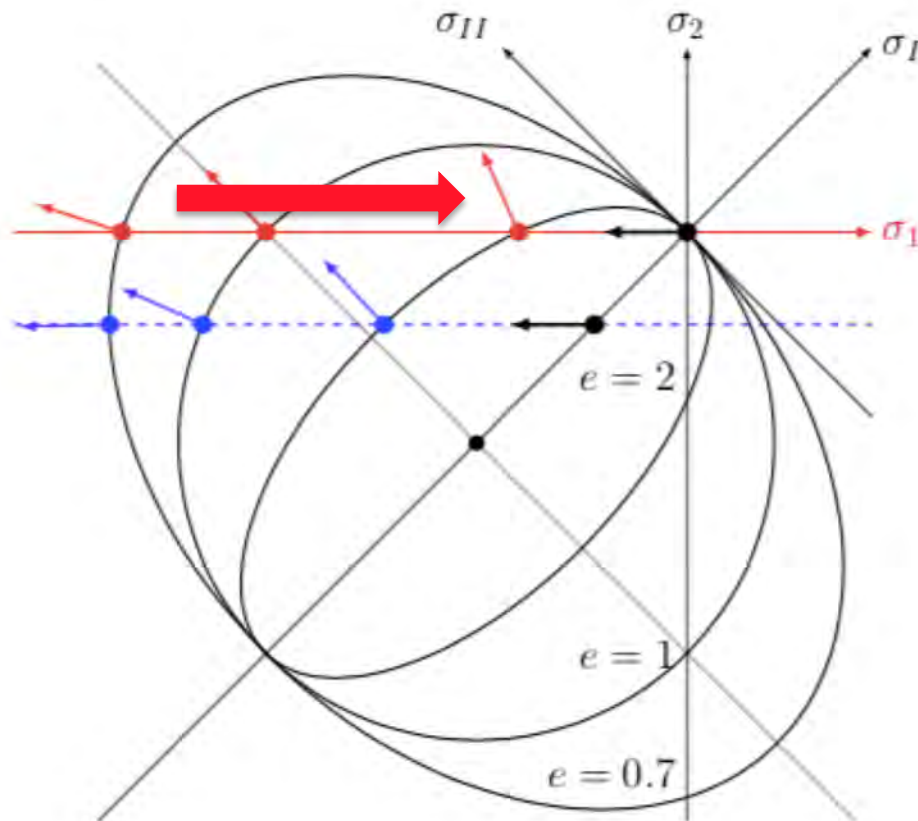
# Axial Loading Test

## Increased Shear Strength ( $e=0.7$ )



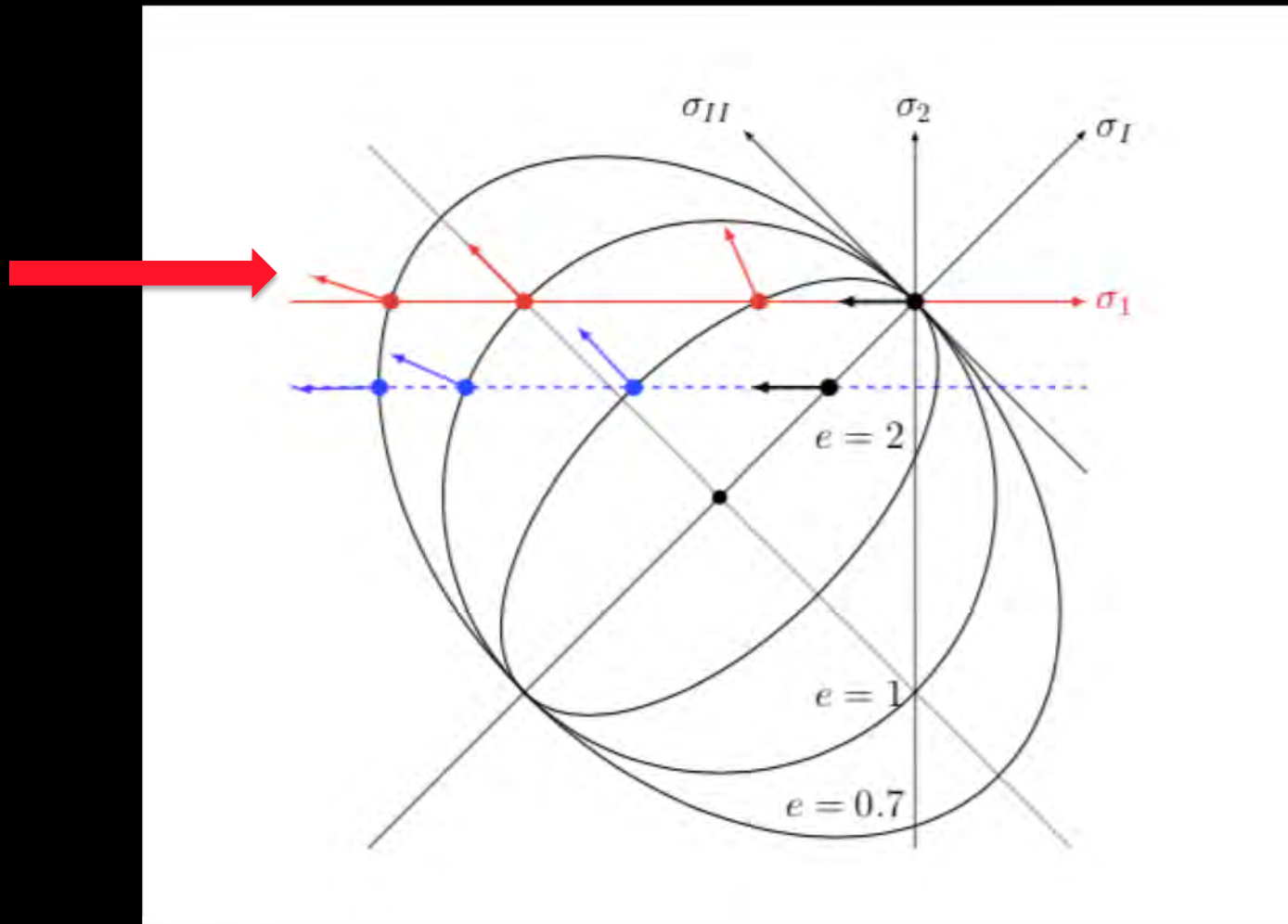
61 degrees

# Axial Loading Test

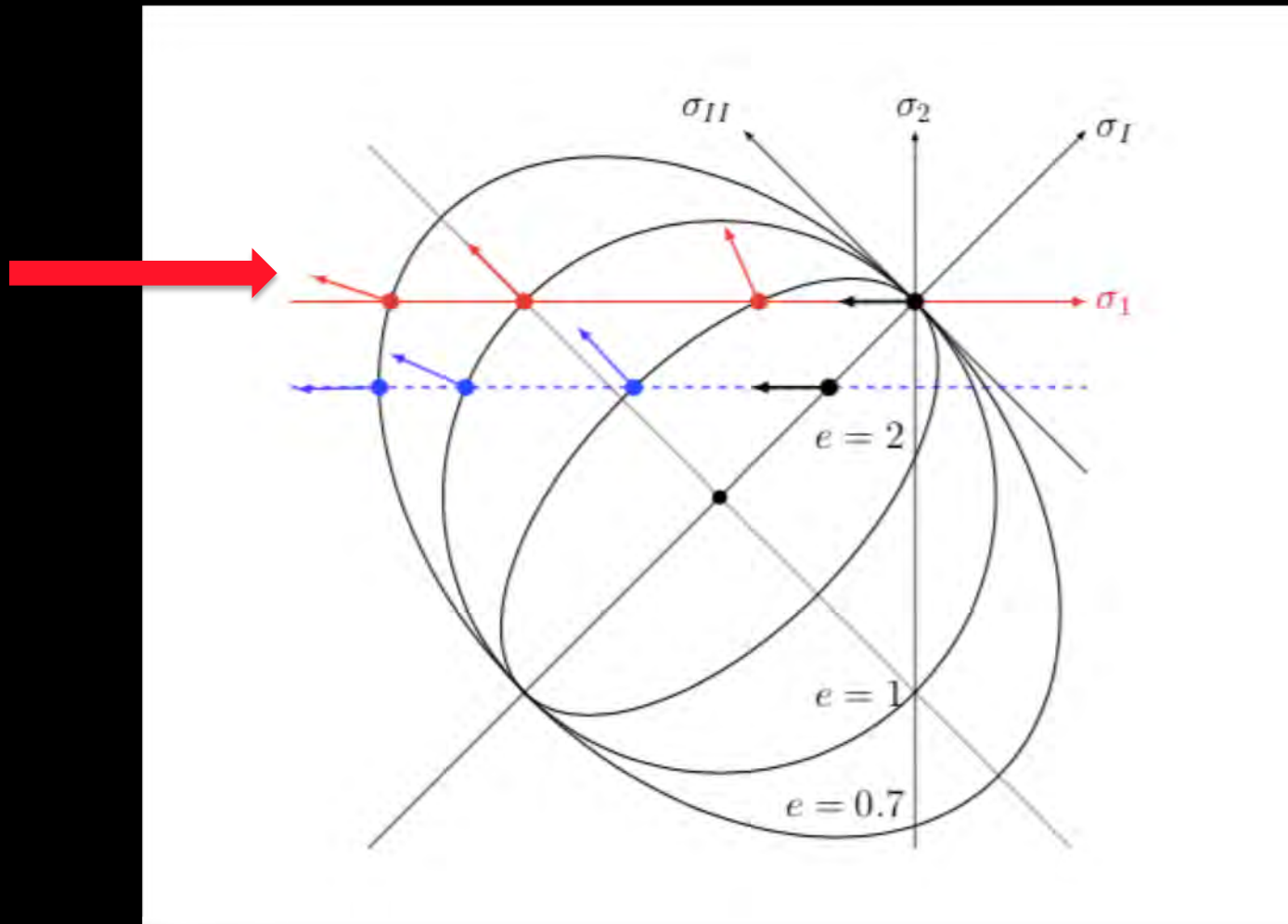




# Axial Loading Test

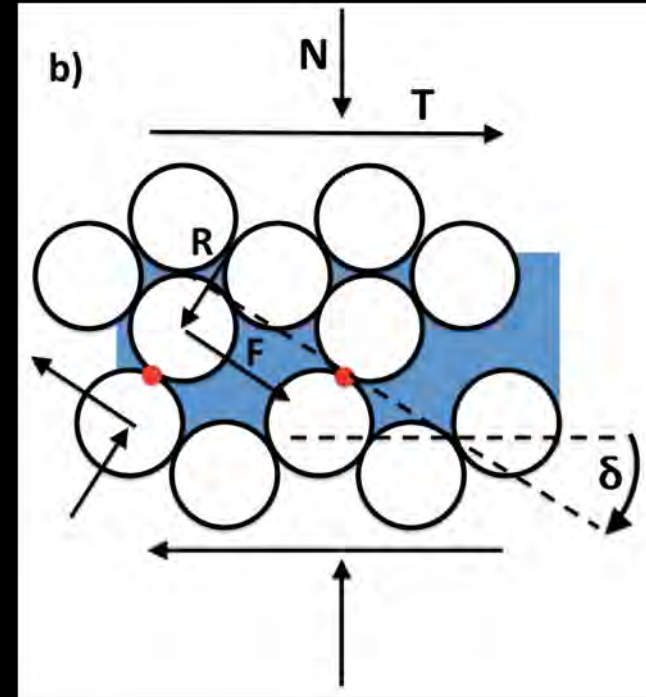
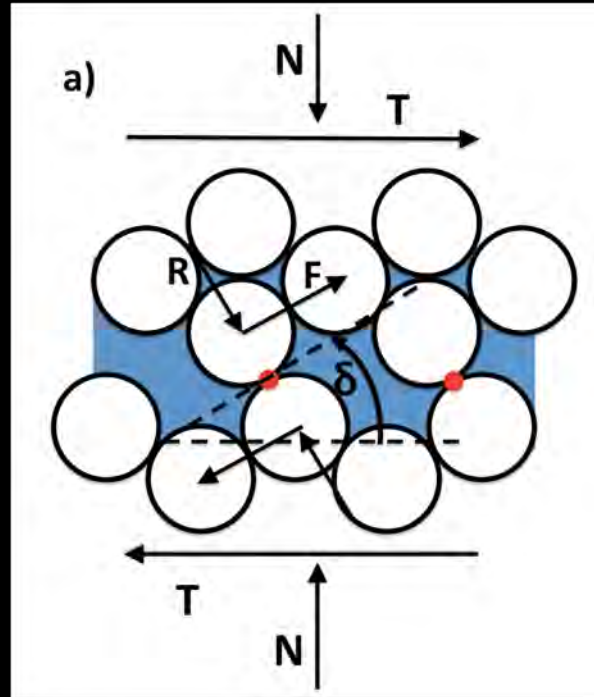
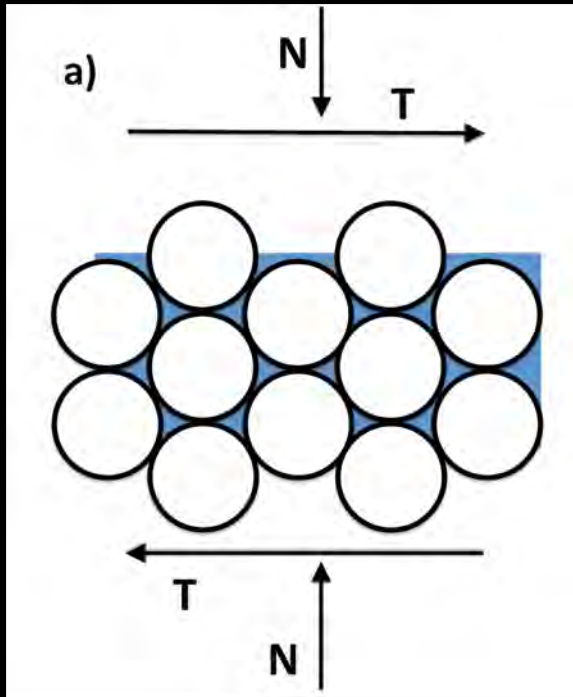


# Axial Loading Test

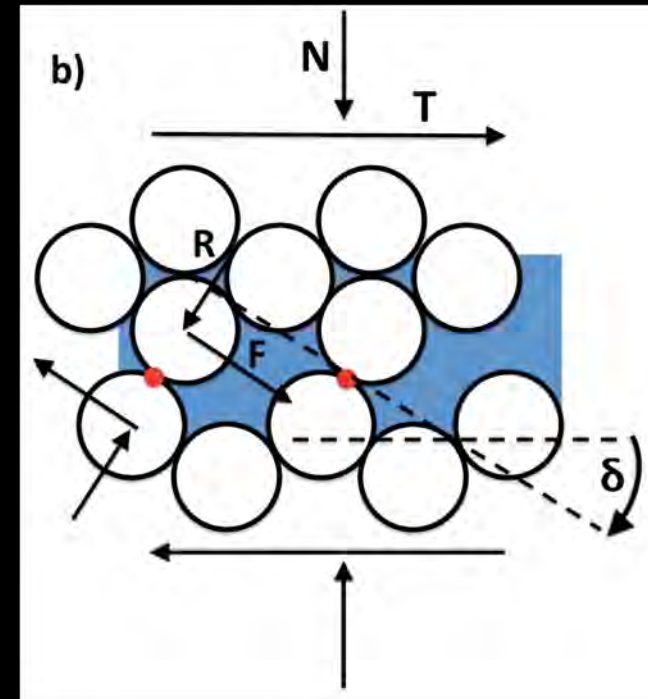
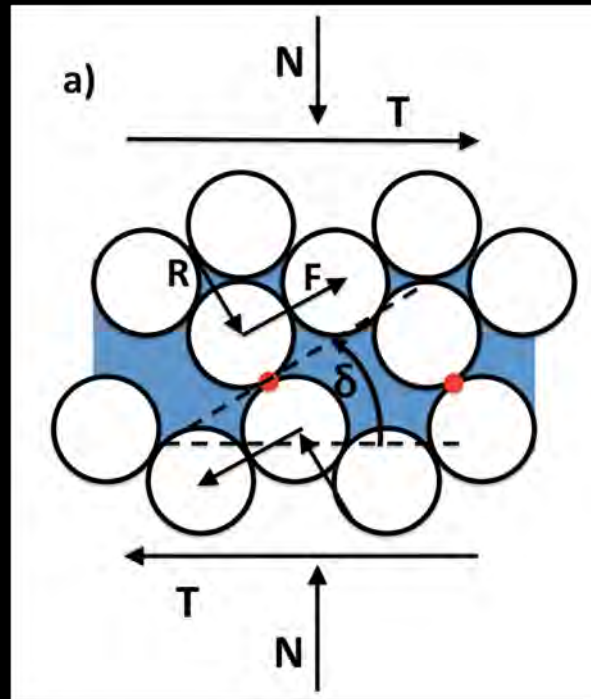
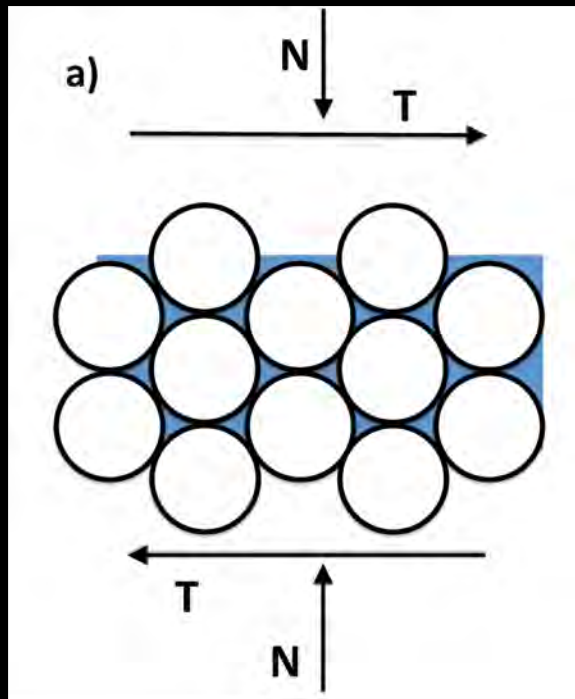


Divergence along ice fracture is set by the shear strength of the ice

# Shear resistance -- Dilatation

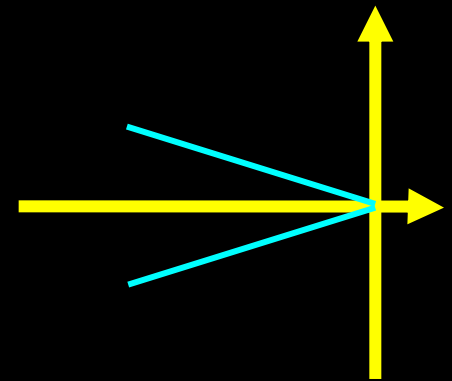
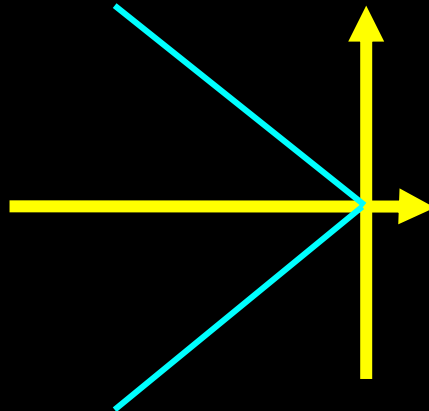
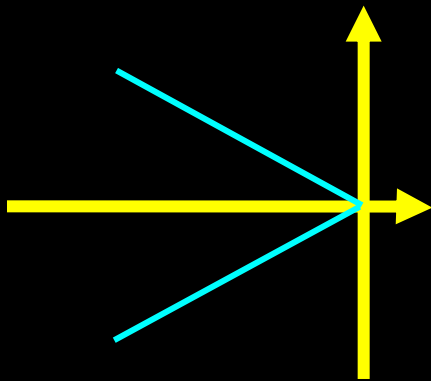
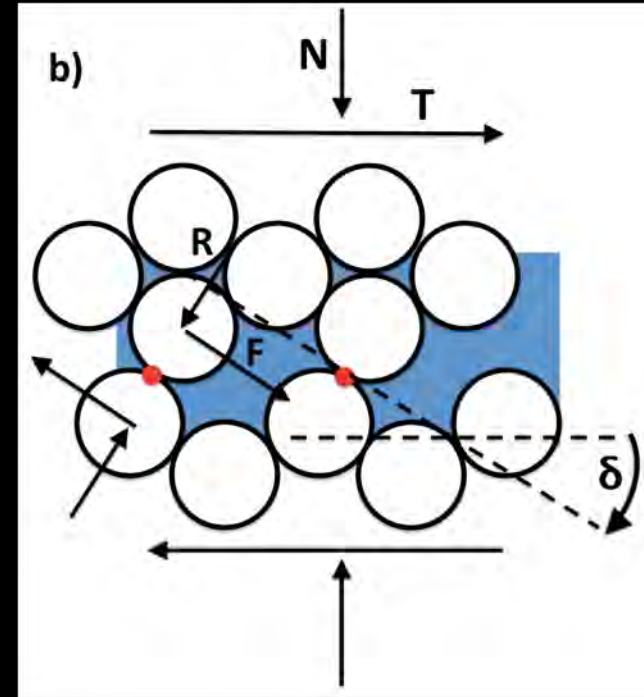
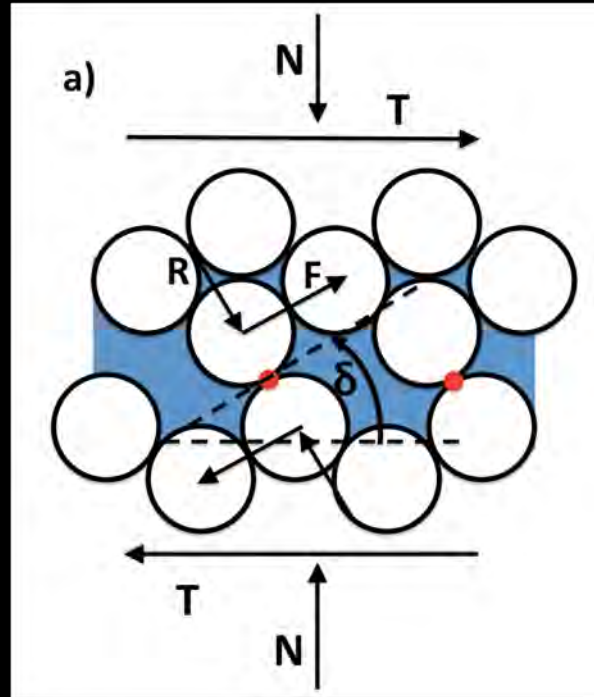
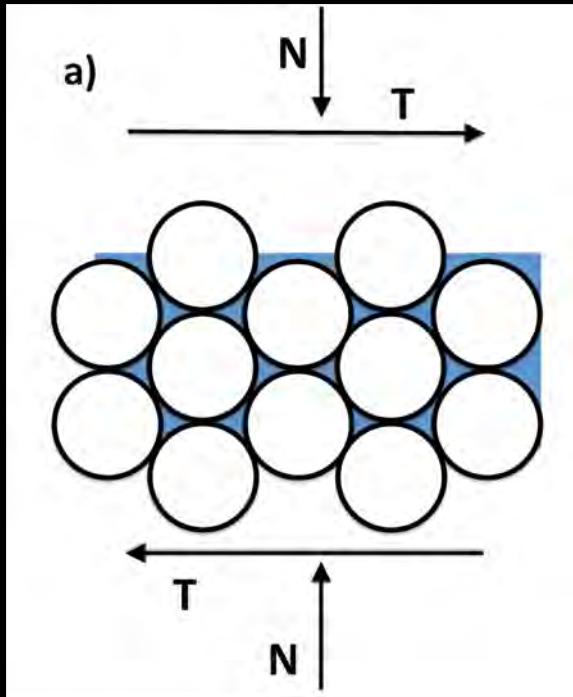


# Shear resistance -- Dilatation



In a granular material:  
high shear resistance leads to divergence  
and  
low shear resistance leads to convergence

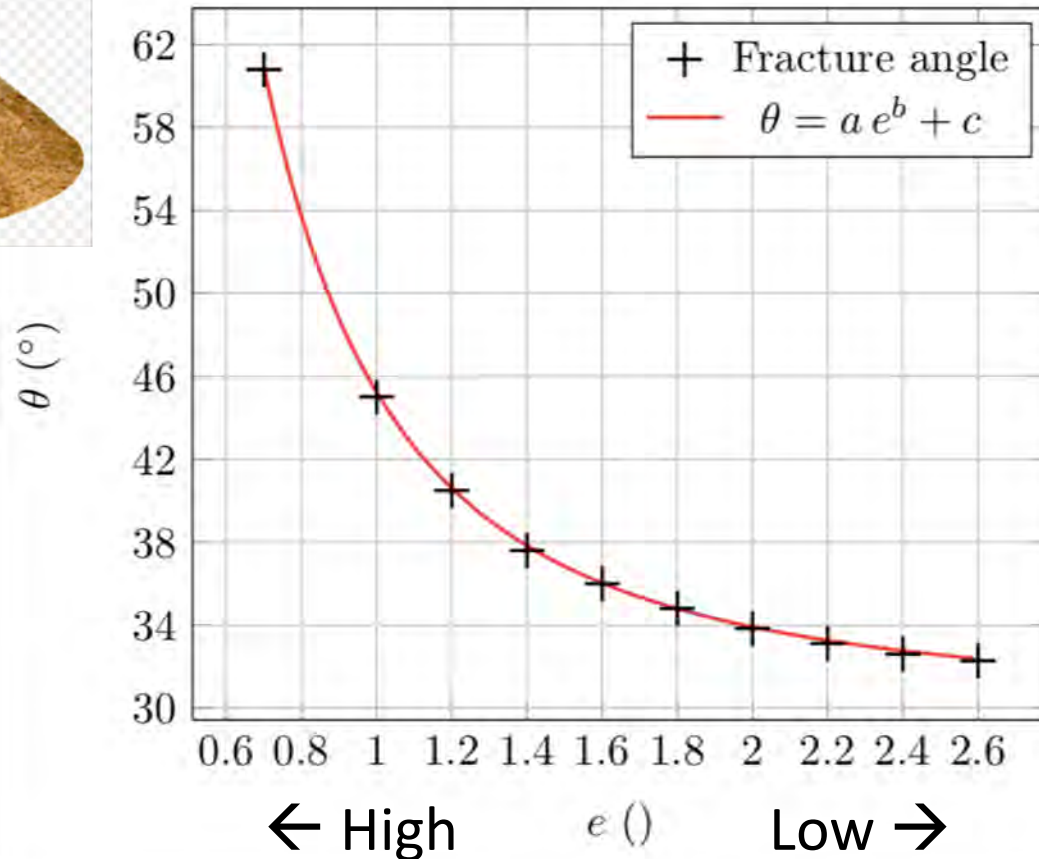
# Shear resistance -- Dilatation



# Angle of Fracture vs Shear Strength



Angle larger  
than observations  
for all shear  
strength



Shear Strength

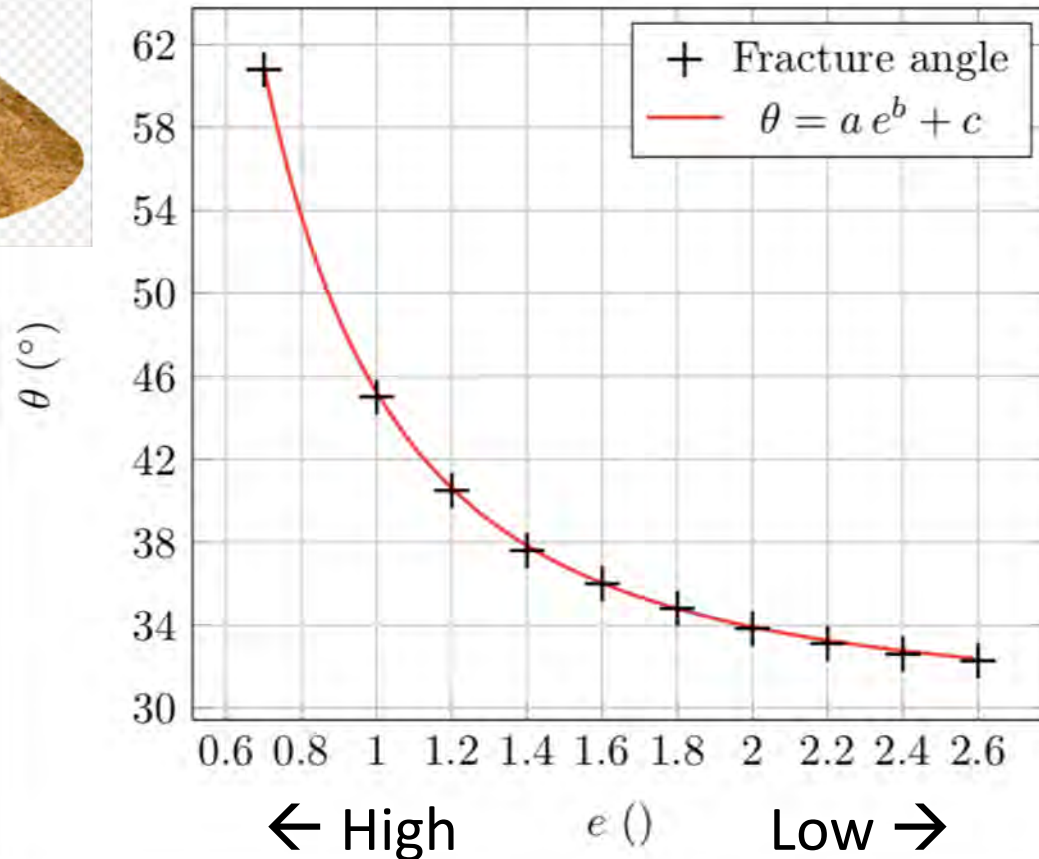




# Angle of Fracture vs Shear Strngth



Angle larger  
than observations  
for all shear  
strength



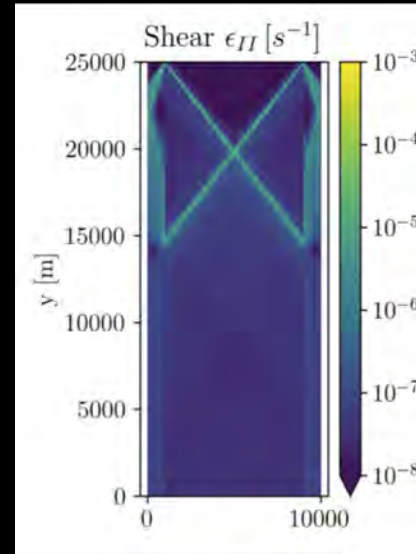
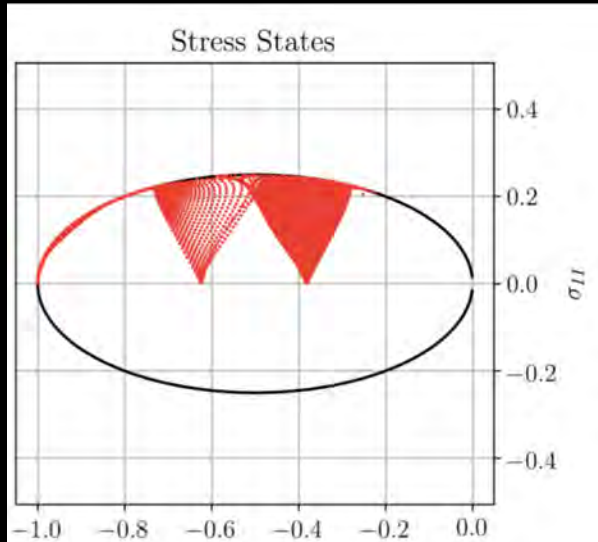
Shear Strength



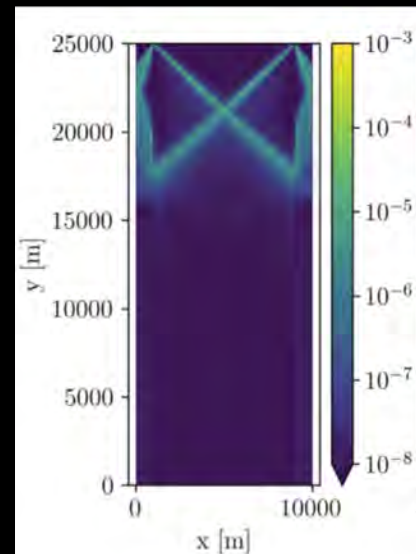
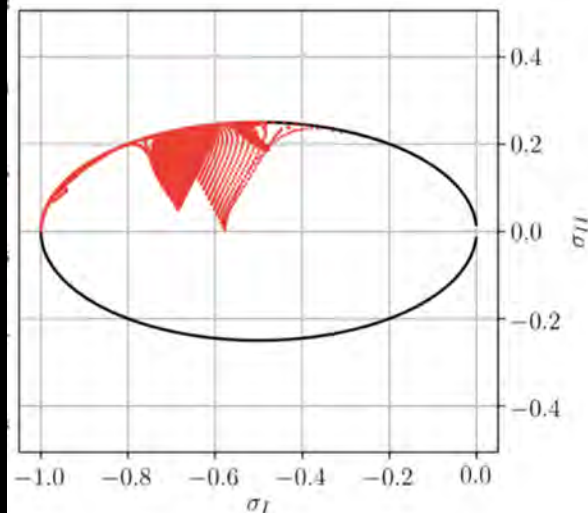
Again contrary to the behavior of a granular material

# Axial Loading Test

## Confining Pressure

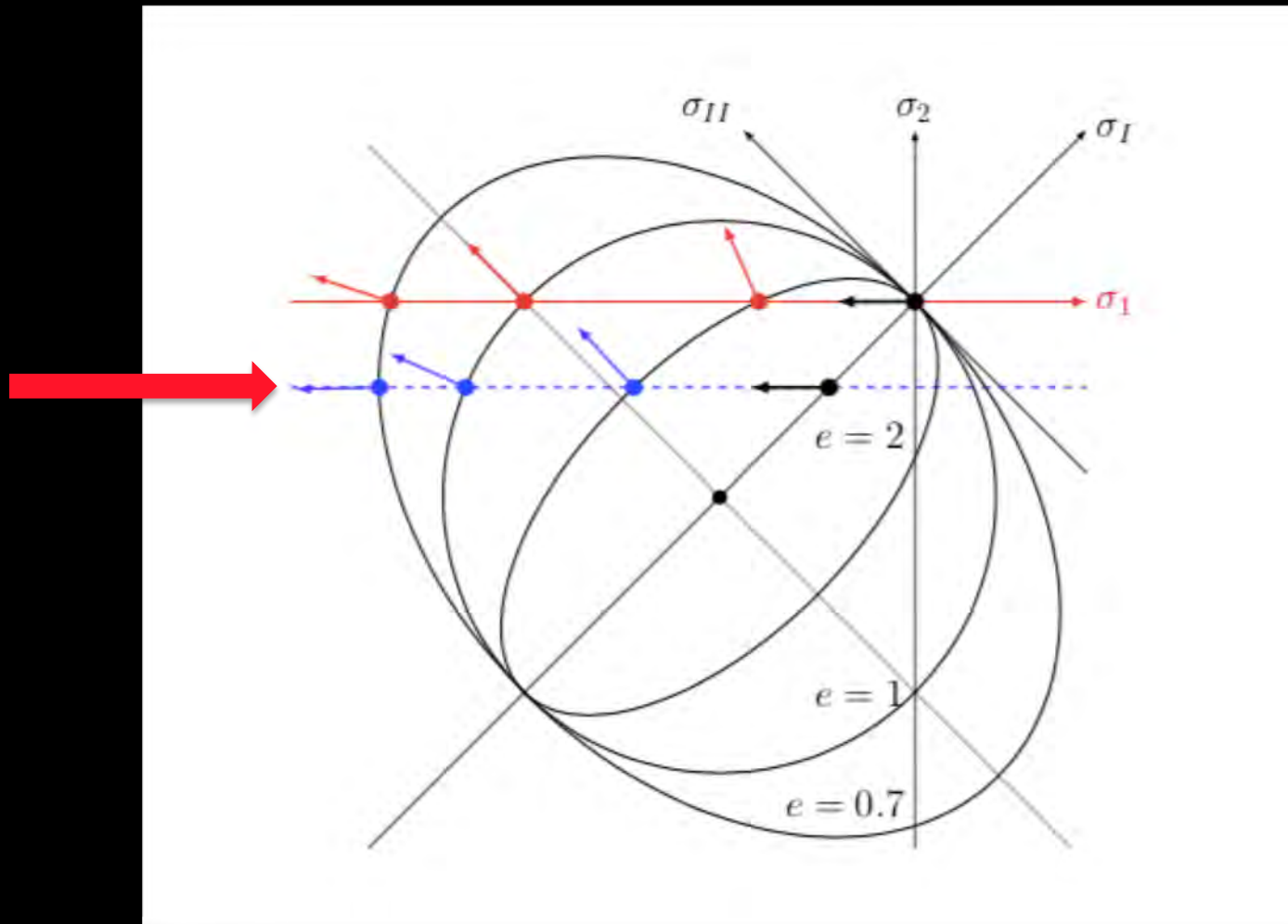


Low confining pressure



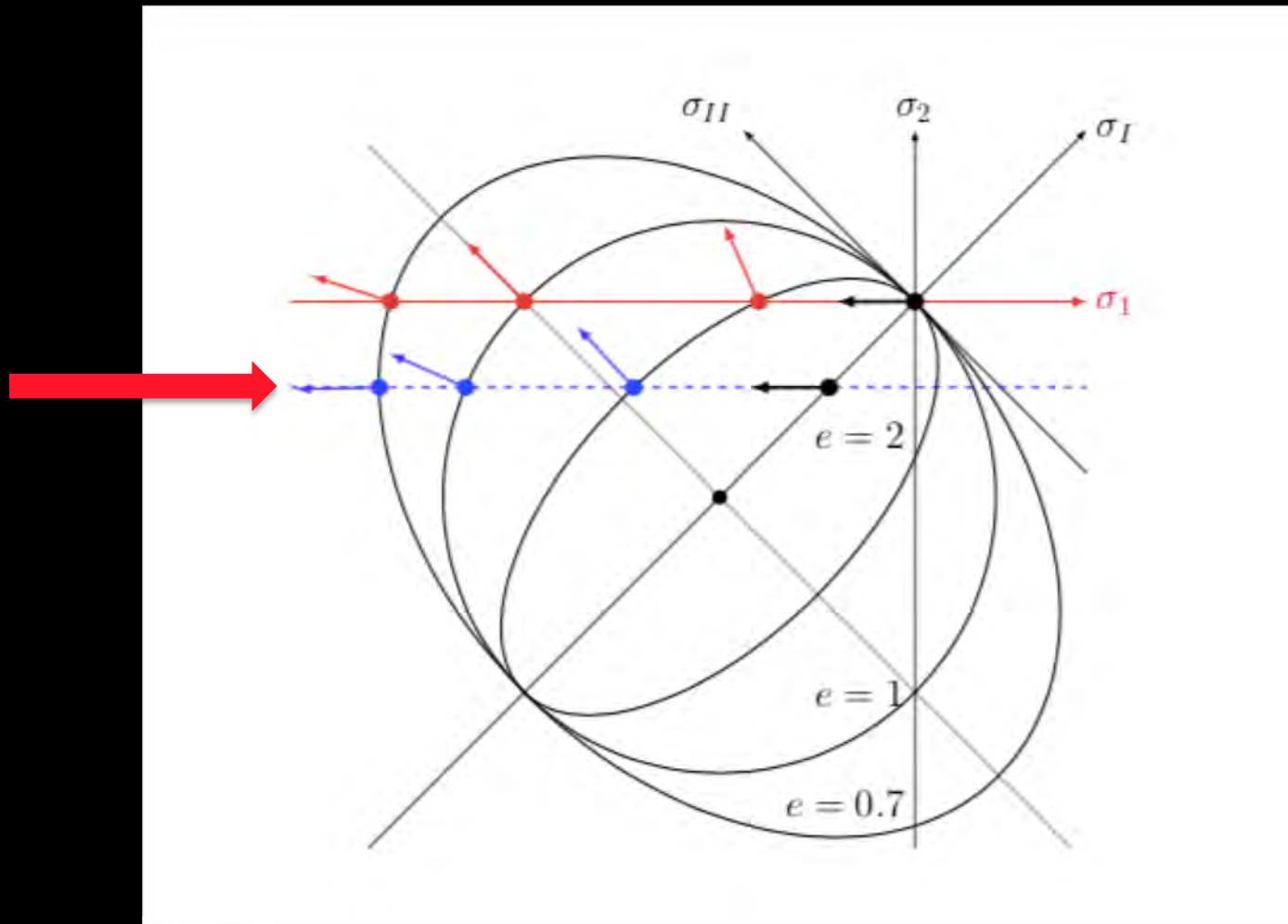
High confining pressure

# Axial Loading Test



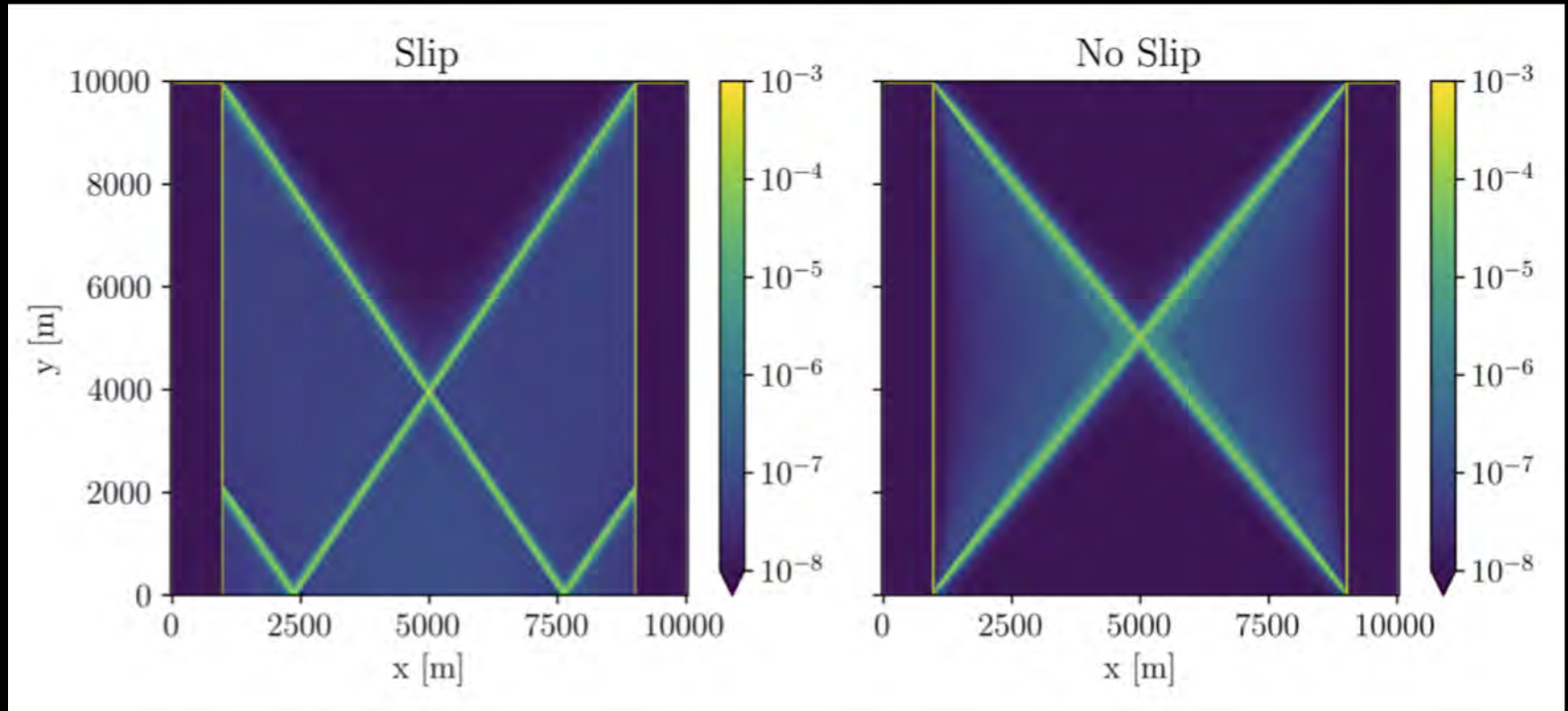
Divergence and angle of fracture depends on the confining pressure

# Axial Loading Test



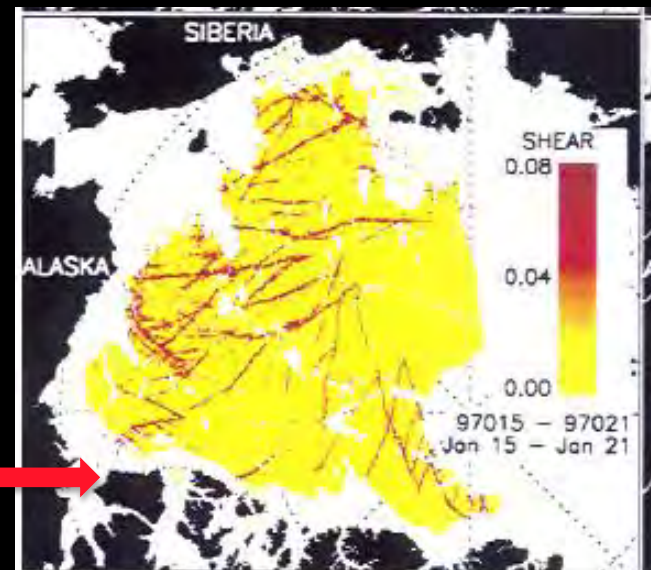
Again contrary to a granular material

# Boundary Conditions



# This re-opens the question of boundary conditions

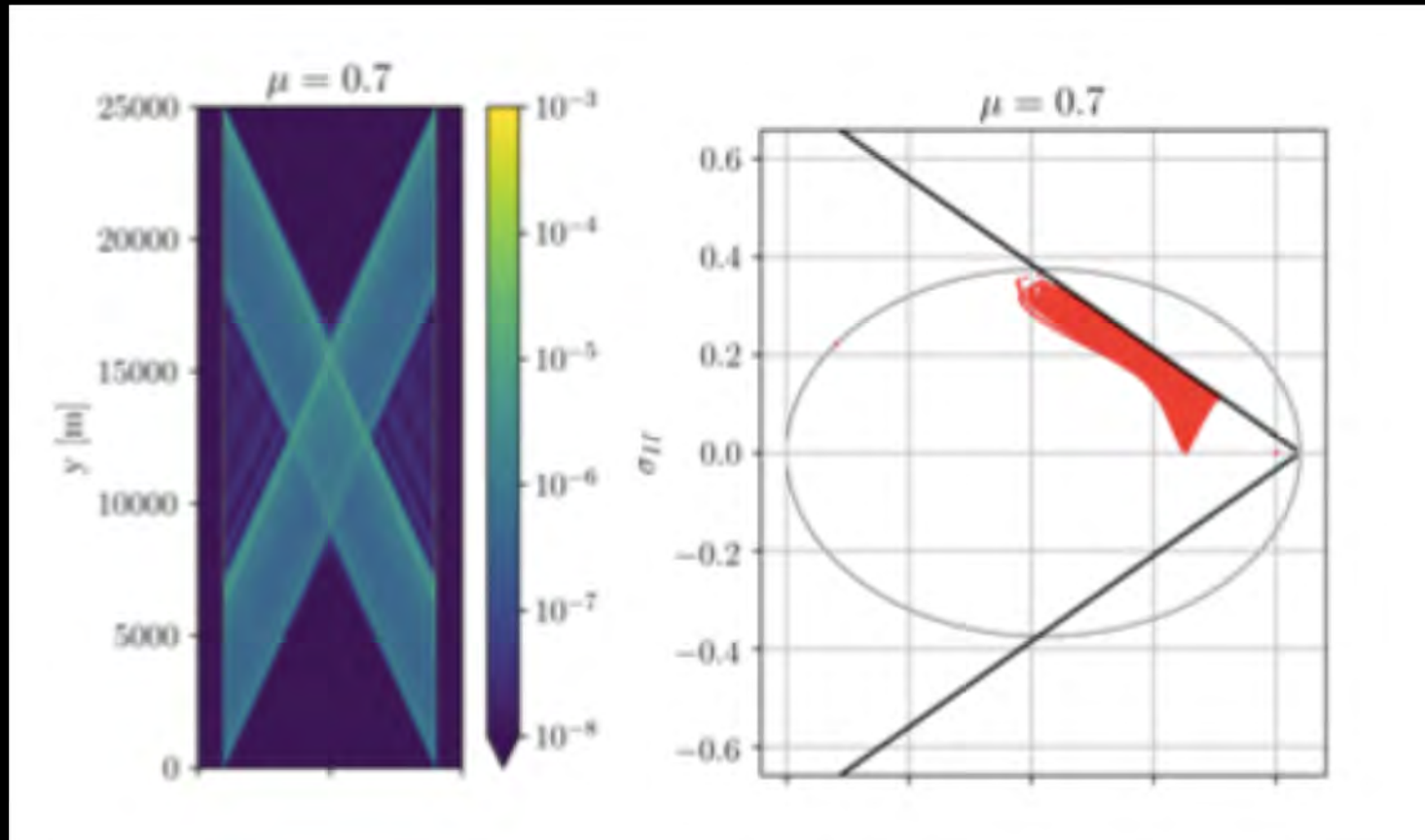
- Currently we use no-slip  $u=v=0$
- A more natural boundary condition is set on the stresses:
  - open boundary: stress free
  - Closed boundary: stress from yield curve





# Axial Loading Test

## Mohr-Coulomb



Angle of fracture is 23 deg in line with theory and RGPS observations

# Conclusions

- The dependence of the fracture angle on shear strength is contrary to that of a granular material.
- The divergence along ice fracture is set by the shear strength contrary to granular material where shear strength and dilatation (divergence) evolve in time and are a function of the distribution of contact normals.
- The angle of fracture depends on the confining pressure contrary to granular material.
- The angle of fracture depends on the choice of boundary condition.

# Way Forward

- Dissipation of energy with a Mohr-Coulomb rheology
- What is the implied flow rule in the when plastic deformation are simulated as elastic deformation with reduced elastic stiffness
- What is the fracture pattern simulated by the plastic constitute relation in the limit where  $\eta$  and  $\zeta$  reach their maximum values

# Constitutive Relations

## Viscous Plastic

- Elastic deformation are simulated as highly viscous (ideal plastic plastic)
- Plastic constitutive relations.
- Macroscopic angle of friction, dilatation and shear strength are related and time evolving.

## Elasto Brittle

- Elastic constitutive relations.
- Plastic deformation are simulated as elastic deformation with a small Elastic Modulus (or spring constant)

# Constitutive Relations

## Viscous Plastic

- Elastic deformation are simulated as highly viscous (ideal plastic plastic)
- Plastic constitutive relations.
- Macroscopic angle of friction, dilatation and shear strength are related to one another time evolving.

## Elasto Brittle

- Elastic constitutive relations.
- Plastic deformation are simulated as elastic deformation with a small Elastic Modulus (or spring constant)

# Constitutive Relations

## Viscous Plastic

- Elastic deformation are simulated as highly viscous (ideal plastic plastic)
- Plastic constitutive relations.
- Macroscopic angle of friction, dilatation and shear strength are related to one another time evolving.

## Elasto Brittle

- Elastic constitutive relations.
- Plastic deformation are simulated as elastic deformation with a small Elastic Modulus (or spring constant)

Discretization (FEM or FD), advection scheme (Lagrangian or Eulerian), dilatation, variable macroscopic angle of friction are not model specific



# Constitutive Relations

$$3 \times 10^{12} \text{ kg/s} \quad \sim 2 \times 10^{12} \text{ kg/s}$$

$$\sigma_{ij} = 2\eta\dot{\epsilon}_{ij} + \left[ (\zeta - \eta)\dot{\epsilon}_{kk} - \frac{P}{2} \right] \delta_{ij},$$

Viscous Plastic

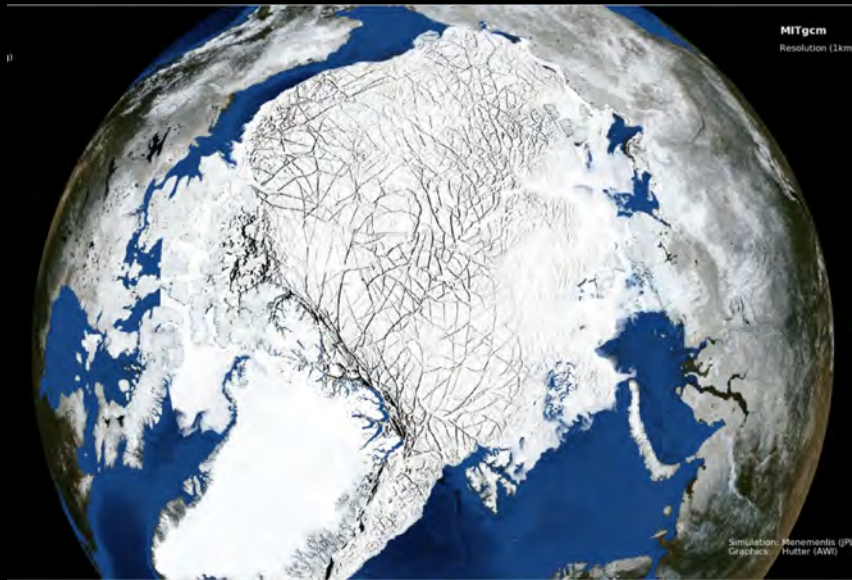
$$\sigma_{ij} = 2G\epsilon_{ij} + \lambda\delta_{ij}\epsilon_{kk}$$

Elasto Brittle

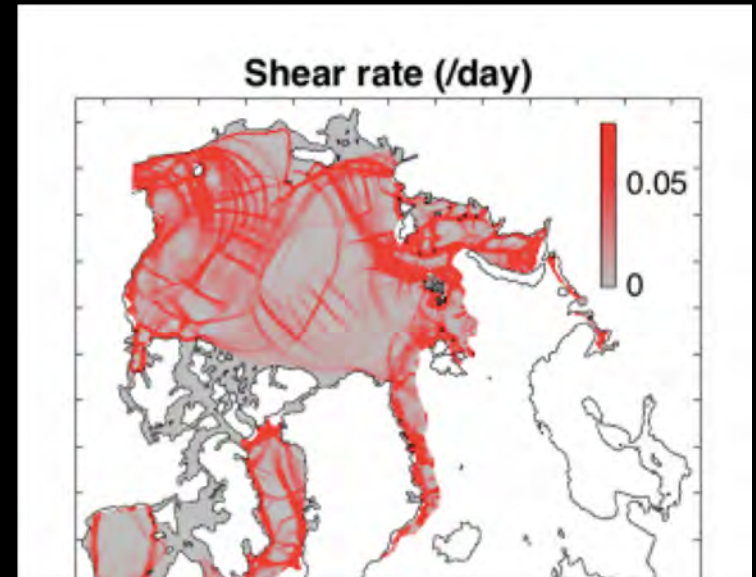
$$8 \times 10^7 \text{ kg/s}^2$$

characteristic time of ~6 hours ( $\sim 2 \times 10^5 \text{ sec}$ )

# VP vs neXtSIM



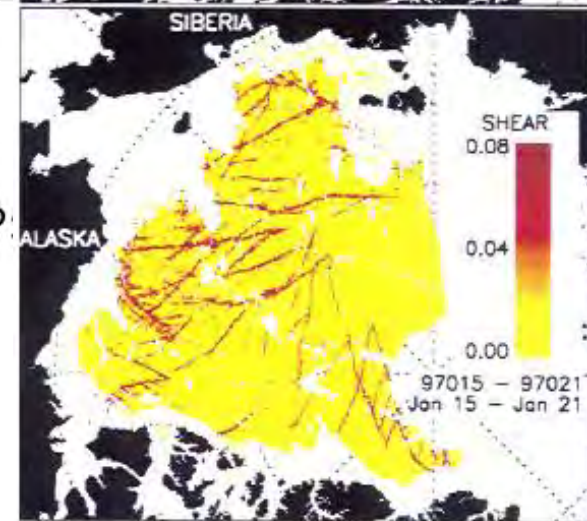
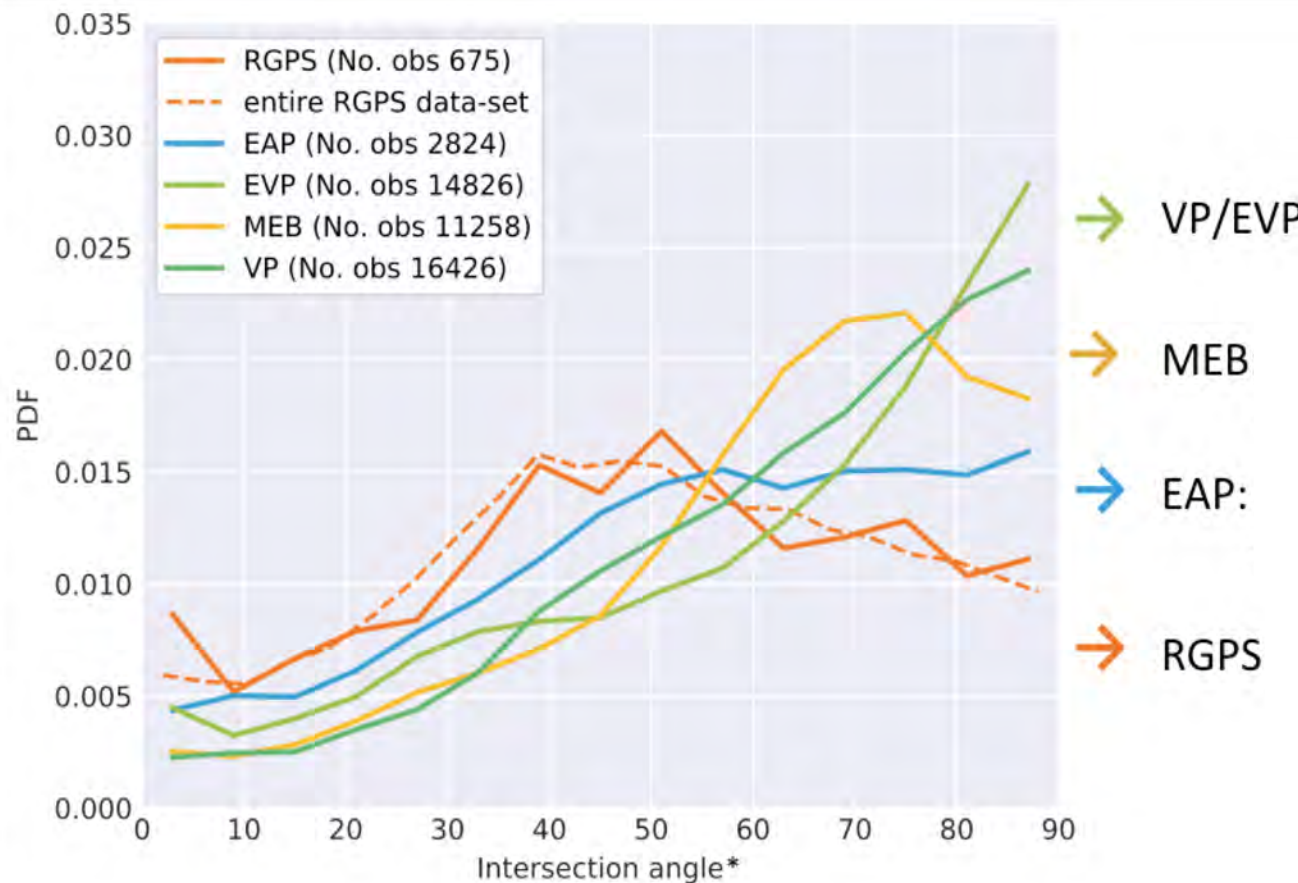
VP, 1km, 2 OL, Hutter



neXtSIM (EB), Rampal et al. 2016

LKFs appear to be a fundamental property of plasticity theory

# Intersection angle of Fracture Lines



Range of intersection angle in line with a MC yield curve with Dilatation and variable macroscopic angle of friction

# Time scale associated with Viscous Deformation

Viscous time scale:  $10^{-4} \text{ day}^{-1}$  (Hibler, 1979)

→ ~30 years

Characteristic time scale for LKFs: hours or day

# Outlook

- Important to continue to use multiple approach. We should encourage diversity rather than converging towards a single approach.
- It generates interesting questions and furthers our understanding all approaches used.

# Outlook

- Use a sea ice rheology that includes all behavior of sea ice: elastic, viscous and plastic.
- Consider both thermal and mechanical stresses inside ice.
- Develop yield criteria based on the vertically dependent internal stress
- Move to Discrete Element Model and Lagrangian advection scheme